Inorganic Chemistry

pubs.acs.org/IC
Article

Multivariate Metal−Organic Framework-5 with 36 Different Linkers

Matthew Burigana,[#] Haoze Wang,[#] Jonas Elmroth Nordlander, and Omar M. Yaghi*

Cite This: *Inorg. Chem.* 2025, 64, 5561−5567
Read Online
ACCESS | Metrics & More | Article Recommendations | Supporting Information

ABSTRACT: We synthesized a series of multivariate metal−organic frameworks (MTV-MOFs) containing 36 different organic linkers with 27 unique functionalities. The functionalities present on the linkers include amine, nitro, halide, naphthalene, alkyne, alkene, alkane, ether, phenyl, pyridine, thiophene, and amide groups. These MTV-MOFs were characterized by powder X-ray diffraction to ensure the MOF-5 connectivity forms, solution-state nuclear magnetic resonance to calculate the final linker incorporations, thermogravimetric analysis to confirm the organic component of the framework, and nitrogen sorption isotherms to measure the porosity and calculate the BET surface areas of each MTV-MOF. Each linker was found to make up between 0.07 and 6.64% of the linkers in the structure, with the total framework mass consisting of 74.8−75.1% linker molecules, compared to 63.9% for the linkers in MOF-5. BET surface areas up to 1,755 m^2/g were observed with 36 linkers present compared to 3,380 m^2/g in MOF-5. Thirty-four of the 36 linkers had linear correlations between the starting ratio and final incorporation, indicating interactions between linkers do not heavily influence the incorporation of other linkers into the final structure.

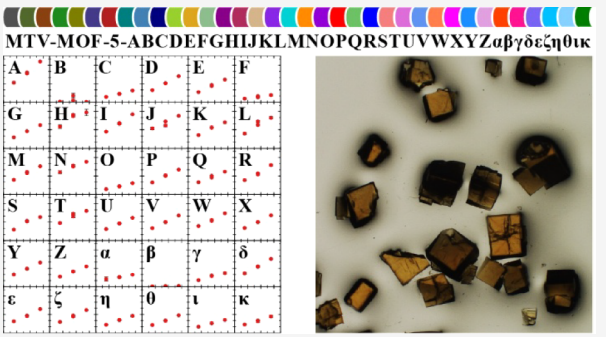

INTRODUCTION

Traditionally, metal−organic frameworks (MOFs) were made with a single linker and secondary building unit (SBU), resulting in pores surrounded by the same functionalities, termed homogeneous pore environments.[1−3] Using multiple linkers with different connectivities allowed reticular chemists to access new topologies and make MOFs with ultrahigh surface areas.[4−10] Linkers with the same connectivity and different functionalities were likely to be nonperiodically distributed throughout a framework though, introducing different functional groups into various pores of the same structure.[11−15] The first multivariate (MTV) MOFs built on this idea, incorporating up to 8 linkers with the same connectivity but different functionalities into one framework based on the MOF-5 backbone.[16] A MOF-5 backbone is the zinc oxide and phenylene units of 1,4-benzenedicarboxylic acid (BDC) that make up MOF-5 without any functionalities present. The resulting MTV-MOFs all contained heterogeneous pore environments, where many different functionalities can surround a single pore. The use of multiple linkers showed increased CO_2/CO selectivity and an increase in hydrogen sorption capacity compared to MOF-5. Later work targeting the development of MTV-MOFs installed up to 10 metals in the SBU of a single MOF, giving a MOF-74 backbone with many metals.[17,18]

Incorporating more linkers will create more types of heterogeneous pore environments in an MTV-MOF. Herein, we report MTV-MOF-5 containing 36 different linkers with 27 unique functionalities, resulting in crystals where each pore can contain a unique environment that is unlikely to be duplicated within the same crystal. The linkers incorporated in MTV-MOF-5 will herein be referred to as A, BDC; B, BDC-NH_2; C, BDC-NO_2; D, BDC-C_4H_4; E, BDC-Br; F, BDC-OC_3H_3; G, BDC-OC_3H_5; H, BDC-OC_3H_7; I, BDC-OC_4H_7; J, BDC-OC_4H_9; K, BDC-$O_2C_3H_7$; L, BDC-OC_5H_9; M, BDC-$O_2C_4H_9$; N, BDC-OC_7H_7; O, BDC-OC_6H_6N; P, BDC-OC_8H_9; Q, BDC-OC_8H_9; R, BDC-OC_7H_8N; S, BDC-OC_9H_{11}; T, BDC-$O_2C_9H_{11}$; U, BDC-$OC_{11}H_{15}$; V, BDC-$O_3C_9H_{11}$; W, BDC-$OSBrC_4H_4$; X, BDC-NOC_2H_4; Y, BDC-NOC_5H_{10}; Z, BDC-NOC_8H_8; *α*, BDC-$(Cl)_2$; *β*, BDC-$(OC_3H_3)_2$; *γ*, BDC-$(OC_3H_5)_2$; *δ*, BDC-$(OC_3H_7)_2$; *ε*, BDC-$(OC_4H_7)_2$; *ζ*, BDC-$(OC_4H_9)_2$; *η*, BDC-$(OC_7H_7)_2$; *θ*, BDC-$(O_2C_9H_{11})_2$; *ι*, BDC-$(O_3C_9H_{11})_2$; and *κ*, BDC-$(OSBrC_4H_4)_2$. We describe the structure of the MOF backbone formed, the porosity of each MTV-MOF, and how each linker varies its incorporation relative to the starting ratio of each linker.

EXPERIMENTAL SECTION

The corresponding volumes of 0.0416 M linker solution in *N*,*N*-diethylformamide (DEF) for each of the 4 MTV-MOF-5 samples (I, II, III, IV), listed in Table S1, were mixed for a total

Received: January 2, 2025
Revised: March 2, 2025
Accepted: March 6, 2025
Published: March 10, 2025

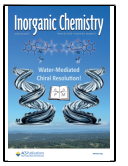

Scheme 1. 36 Linkers Used to Make MTV-MOF-5-ABCDEFGHIJKLMNOPQRSTUVWXYZ*αβγδεζηθικ*, Termed (I), (II), (III), and (IV)

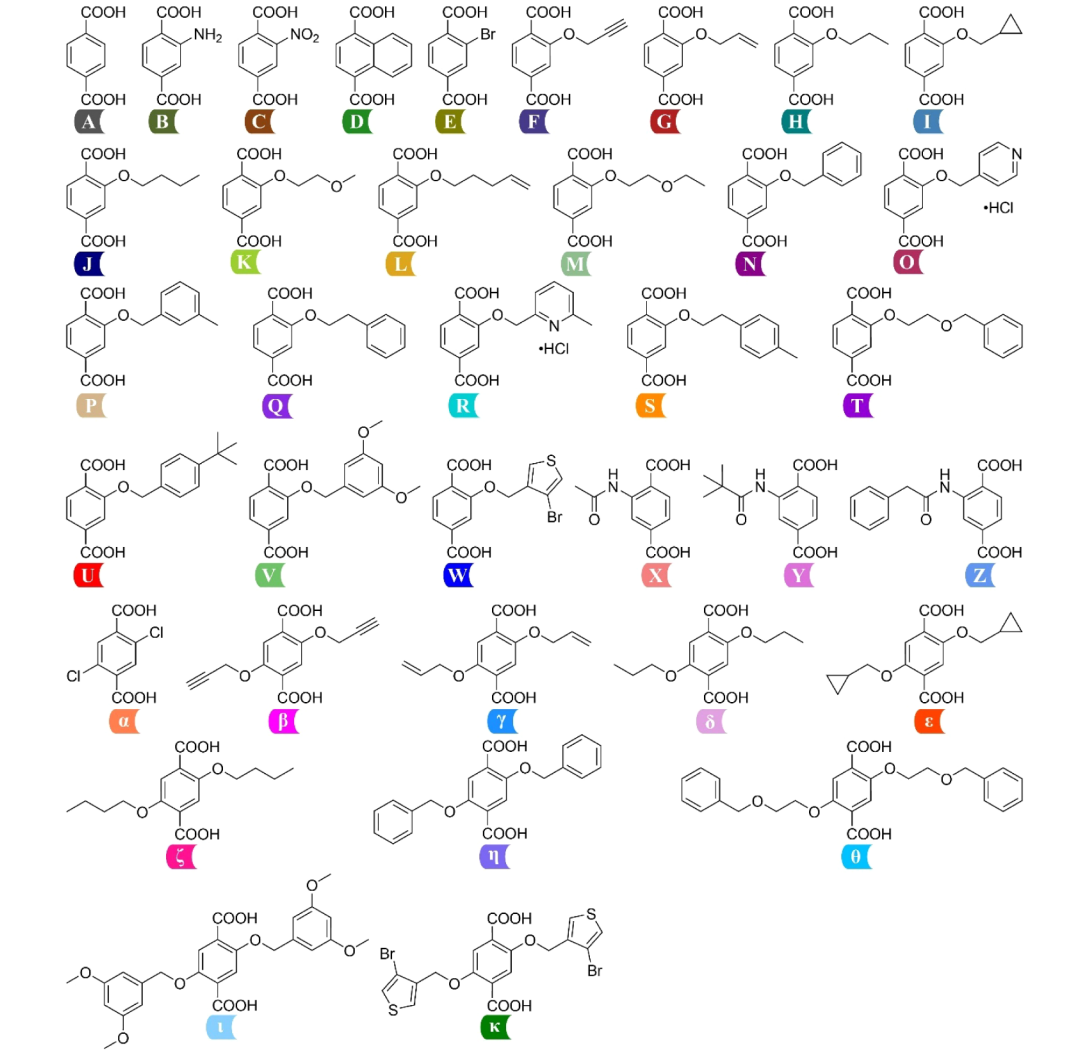

volume of 10 mL in a 20 mL scintillation vial. Zinc nitrate hexahydrate (365.2 mg, 1.227 mmol) was added, and the mixture was sonicated for 10 min to dissolve the remaining solids. Once all the solids were dissolved, the mixture was vortexed and heated at 100 °C for 48 h. The solution was cooled to room temperature then the solvent was exchanged 6 times with anhydrous *N*,*N*-dimethylformamide (DMF) over 2 days to wash the brown MOF crystals. The crystals were stored in anhydrous DMF until preparation for activation. To prepare for activation, the solvent was exchanged 6 times with anhydrous dichloromethane (DCM) over 2 days. The DCM was decanted, and the MOFs were activated at 120 °C for 20 h *in vacuo*.

RESULTS AND DISCUSSION

Crystals of MTV-MOF-5 were obtained by adding $Zn(NO_3)_2 \cdot 6H_2O$ to a DEF solution containing the acid form of each linker and heating at 100 °C for 48 h. The resulting crystals were characterized by powder X-ray diffraction (PXRD), ^1H nuclear magnetic resonance (NMR) on acid digested solutions of the crystals, thermogravimetric analysis (TGA), and nitrogen gas sorption at 77 K to assess their crystallinity, linker ratios, thermal stability, and porosity, respectively. Four MTV-MOF-5 samples were prepared where each reaction contained different starting percentages of the linkers, structures shown in Scheme 1, to assess how the final composition is affected by the starting linker ratio. Specifically, MTV-MOF-5(I) had an equal percent of each linker in the starting solution (2.78%), and MTV-MOF-5(II), (III), and (IV) each had one-third of the linkers at a higher concentration (3.78%), one-third at a lower concentration (1.78%), and one-third remained at 2.78%. The exact percentages used for each linker with the corresponding final incorporation are listed in Table S2. To determine how the synthesis conditions affect the properties of MOF-5, a MOF-5 sample was also prepared using the same linker to metal ratio used for the MTV samples.

The crystallinity of each MTV-MOF is evident by the PXRD shown in Figure 1a, where each crystal gave sharp diffraction peaks matching the simulated and experimental patterns of MOF-5. Despite this high crystallinity, no MTV-MOF-5 sample was able to be characterized by single crystal XRD at

https://doi.org/10.1021/acs.inorgchem.5c00015
Inorg. Chem. 2025, 64, 5561−5567

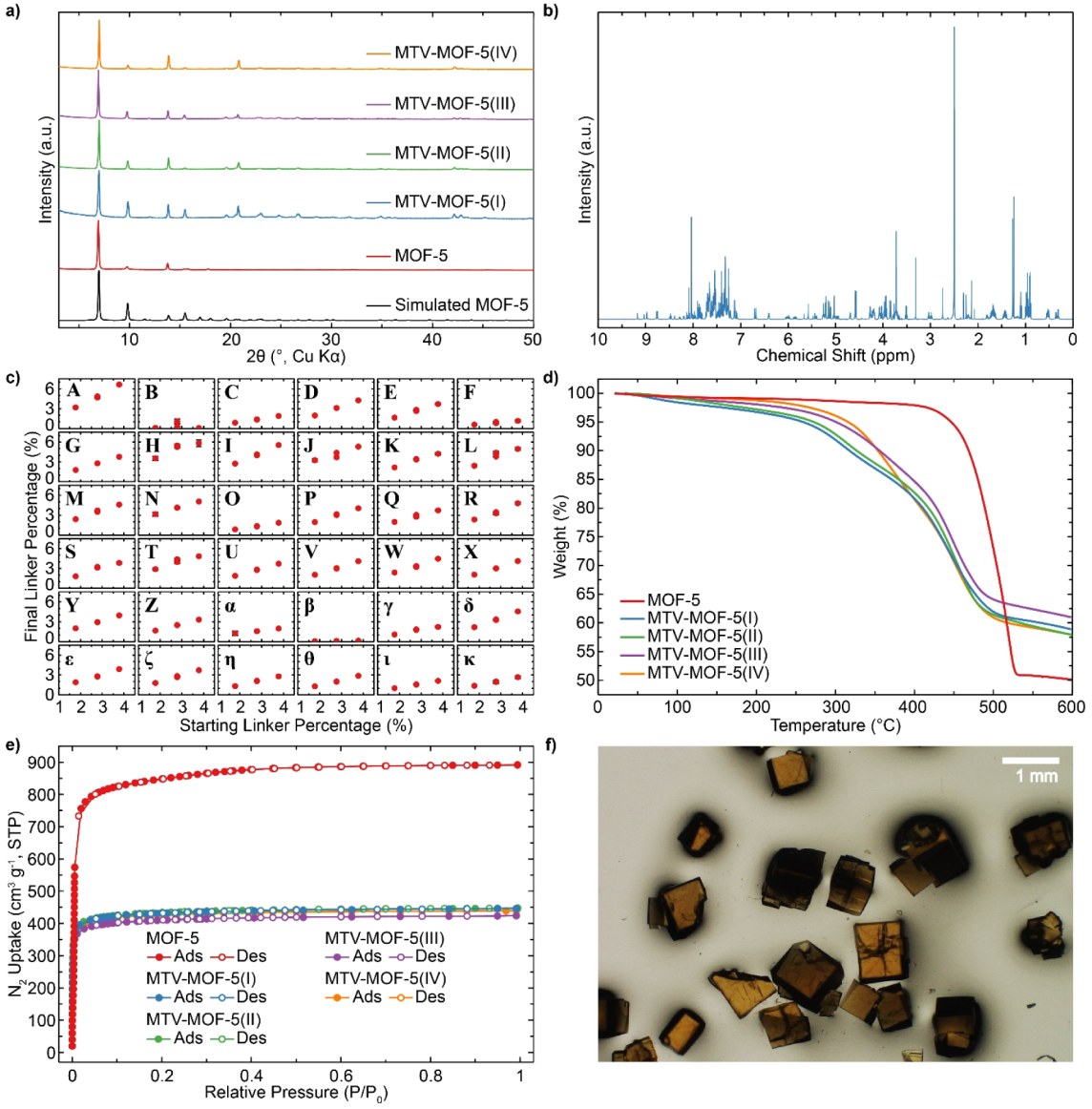

Figure 1. (a) PXRD patterns of MTV-MOF-5 with 36 linkers compared to MOF-5 and a simulated MOF-5 structure. (b) ^{1}H NMR spectrum of digested MTV-MOF-5(I). (c) Final linker percentages compared to the starting linker percentage in the solution. (d) TGA of the decomposition of each MTV-MOF in nitrogen up to 600 °C compared to MOF-5. (e) N_2 isotherms of each MTV-MOF at 77 K. (f) Microscope image of MTV-MOF-5(I) crystals. Scale bar is set to 1 mm.

either 100 or 290 K.[19] The functional groups on each linker were not distributed periodically throughout the crystal and caused diffuse scattering in the measurement, which obscured too many reflections to allow even the unit cell to be solved. Increasing the measurement temperature to 290 K also did not reduce the diffuse scattering enough to allow a structure to be solved. The good agreement between the PXRD of each MTV-MOF-5 sample and the experimental and simulated PXRD of MOF-5 show a MOF-5 backbone is formed with some distortion of the unit cell from the large functional groups on many linkers. Rietveld refined PXRD for each MTV sample are shown in Figures S7−S11, indicating a slight decrease in the unit cell size for each MTV-MOF compared to MOF-5.

To determine the linker ratios, the crystals were evacuated at 120 °C under vacuum (0.05 Torr) for 20 h to remove any remaining guest molecules then digested in 0.4% DCl in D_2O and DMSO-d_6 prior to measuring ^{1}H NMR. An example of the resulting spectrum for MTV-MOF-5 (I) is shown in Figure 1b. The spectra for each MTV-MOF are shown in Figures S1−S5. The relative linker ratios were calculated based on the ^{1}H NMR integration of chemical shifts assigned to each unique linker. Unfortunately, many chemical shifts overlapped so the incorporations were calculated based on a single chemical shift that did not overlap or the chemical shift with the least complex overlapping peaks to simplify calculations and reduce the error of the reported value. The chemical shifts assigned to each linker and its overlaps, if present, are shown in Figure 2 and tabulated in Table 1.

Overall, 28 linkers had at least one distinct chemical shift that could be used to calculate its incorporation, 7 linkers (B, H, J, T, δ, ζ, and κ) needed to be calculated based on a chemical shift with one overlap, and 1 linker (N) was calculated based on a chemical shift with two other overlapping signals. Linker B had an overlapping doublet with a doublet from linker E (Figure 2b). Linkers H and J had overlapping triplets with triplets from linkers δ and ζ, respectively (Figure

https://doi.org/10.1021/acs.inorgchem.5c00015
Inorg. Chem. 2025, 64, 5561−5567

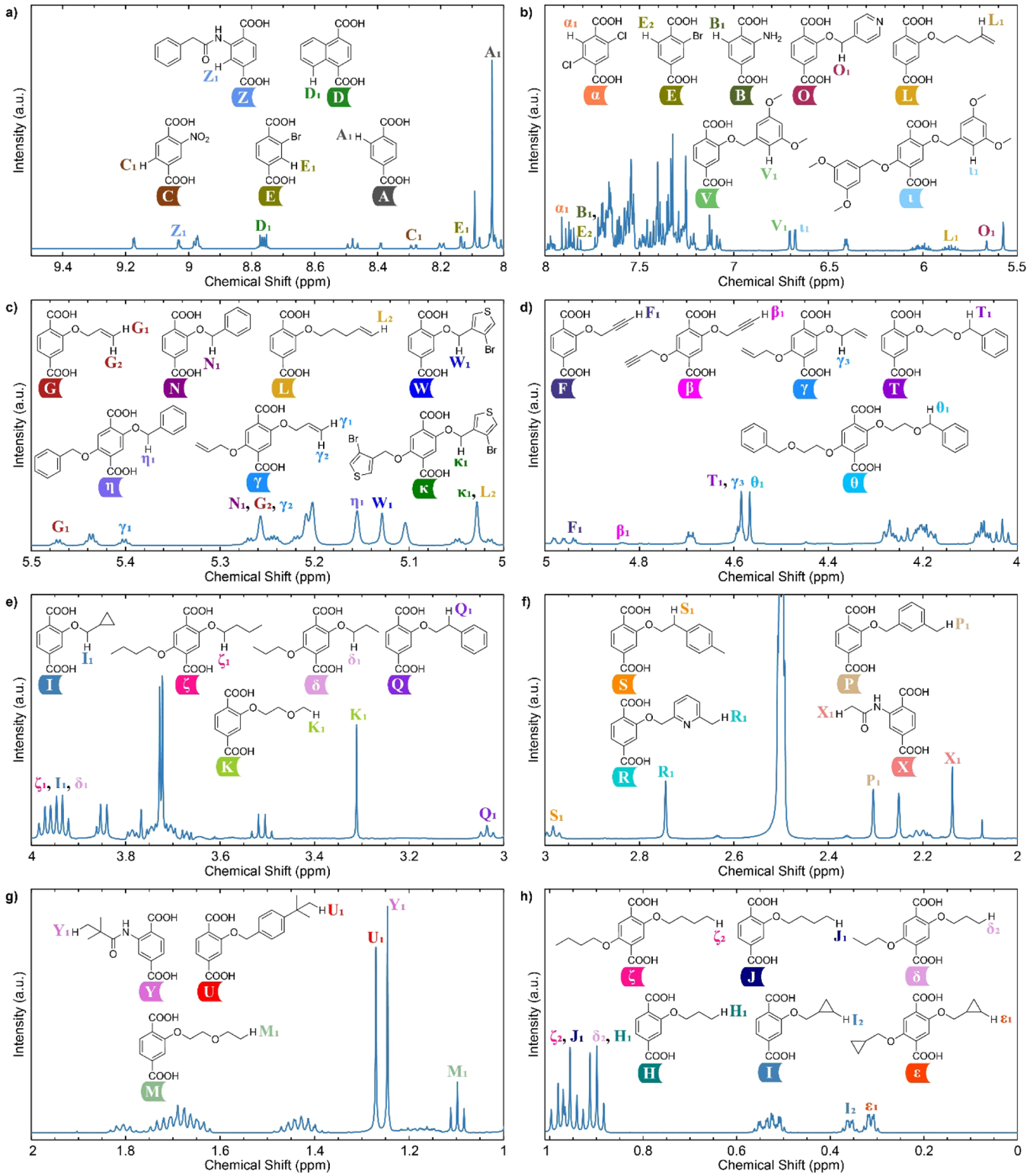

Figure 2. ^{1}H NMR spectrum of MTV-MOF-5(I) from (a) 9.5−8 ppm, (b) 8−5.5 ppm, (c) 5.5−5 ppm, (d) 5−4 ppm, (e) 4−3 ppm, (f) 3−2 ppm, (g) 2−1 ppm, and (h) 1−0 ppm. Spectra are labeled to show which hydrogen(s) on each linker the chemical shifts correspond to, the chemical shifts used to calculate the final linker incorporations, and which hydrogens have overlapping chemical shifts.

2h). Linker T had a singlet that overlapped with a doublet of triplets from linker γ (Figure 2d). Linkers δ and ζ had triplets with signals that overlapped with a doublet from linker I (Figure 2e). The doublet of linker I overlapped such that half was added to the signal of linker δ and half added to linker ζ, allowing the total signal of linker I normalized to 1 hydrogen to be subtracted from each of those signals despite the doublet of linker I corresponding to 2 hydrogens. Linker κ had an overlapping singlet with half of a doublet of doublets from linker L (Figure 2c). The *trans* alkene hydrogen of linker L splits into a doublet of doublets with a large coupling constant, 17.2 Hz, causing only half the signal to overlap with the singlet

https://doi.org/10.1021/acs.inorgchem.5c00015
Inorg. Chem. 2025, 64, 5561−5567

Table 1. Chemical Shift, Multiplicity, and Overlapping Hydrogens for Each Signal Used to Calculate the Linker Ratios from ^{1}H NMR

Linker Hydrogen	Chemical Shift (ppm)	Multiplicity	Number of Hydrogens	Overlapping Linker Hydrogen(s)
A_1	8.04	s	4	
B_1	7.82	d	1	$1 \times E_2$
C_1	8.28	d	1	
D_1	8.79	dd	2	
E_1	8.14	d	1	
F_1	4.95	d	2	
G_1	5.48	dd	0.5	
H_1	0.99	t	3	$6 \times \delta_2$
I_2	0.37	m	2	
J_1	0.92	t	3	$6 \times \zeta_2$
K_1	3.31	s	3	
L_1	5.87	ddt	1	
M_1	1.10	t	3	
N_1	5.27	s	2	$1 \times G_2$, $1 \times \gamma_2$
O_1	5.66	s	2	
P_1	2.31	s	3	
Q_1	3.05	t	2	
R_1	2.74	s	3	
S_1	2.99	t	2	
T_1	4.58	t	2	$4 \times \gamma_3$
U_1	1.28	s	9	
V_1	6.72	d	2	
W_1	5.13	s	2	
X_1	2.14	s	3	
Y_1	1.25	s	9	
Z_1	9.03	d	1	
α_1	7.91	s	2	
β_1	4.85	d	4	
γ_1	5.40	dt	1	
δ_1	3.93	t	4	$1 \times I_1$
ε_1	0.33	m	4	
ζ_1	3.97	t	4	$1 \times I_1$
η_1	5.16	s	4	
θ_1	4.56	s	4	
ι_1	6.69	d	4	
κ_1	5.04	s	4	$0.5 \times L_2$

of linker κ and the correction to calculate for the incorporation of linker κ only accounts for half of the one hydrogen present for linker L. The fact that alkene hydrogens have doublets of doublets with large coupling constants was also used to calculate the incorporations of linkers G, γ, and N (Figure 2c). Half the doublet of doublet signals for linkers G and γ overlap, so their incorporations were calculated based on the half of the signal present without any interference, normalized by 0.5 and 1 hydrogen for G and γ, respectively. Linker N had an overlapping singlet with a doublet of doublets from linker G and from half a doublet of doublets from linker γ, so its incorporation was corrected by the normalized signal of 1 hydrogen from linker G and one hydrogen from linker γ.

The calculated linker compositions are shown in Figure 1c, where an approximately linear relationship between the starting and final linker ratio is present for 34 of the 36 linkers, with the exceptions of linkers B and β. In experiments making MTV-MOF-5 with 11 linkers, linker B was observed to have a threshold starting percent, where if linker B was less than 15% in the starting solution, then the final incorporation was nearly zero. Only in cases where the starting percent of linker B was greater than 15% was it incorporated in appreciable quantities in the final MTV-MOF-5 (Figure S32).[20] The largest starting percent used for linker B was 3.78% in II, so the final incorporation remaining near zero matches the expected behavior for linker B. The alkyne functionality of linkers F and β also limited linker incorporation, where linker F is under incorporated but maintains a linear relationship with the starting linker percentage while linker β is under incorporated and does not maintain a linear relationship its starting percentage. Though the chemical shift for linker β is difficult to distinguish in Figure 2d, its signal-to-noise ratio is 10.1, allowing its calculated incorporation to be considered accurate. An enhanced image of the signals of linkers F and β is shown in Figure S6. The presence of linear relationships between the starting and final linker percentages suggests the final composition of an individual linker is independent of final compositions of the other linkers present. Each linker is incorporated relative to its individual starting ratio and is not aided or excluded by the presence of different functionalities on other linkers.

Previous work used solid state NMR (ssNMR) and molecular simulations to solve for the spatial arrangement of linkers in MTV-MOF-5 with up to three functionalities present.[21] This method relied on the decay of pairwise coupling between labeled ^{13}C and ^{15}N atoms on each functionality based on the ratio of ^{13}C signals measured with and without ^{15}N dipolar modulation for a series of different recoupling times. The experimental ratio was then matched to the predicted signal ratios calculated for various possible linker distributions (alternating, random, small clusters, or large clusters) by molecular simulations. This approach was not possible to use with 36 linkers because the pairwise coupling between specific ^{13}C and ^{15}N atoms would be too infrequent to cause a detectable difference in the ssNMR signal. The ^{13}C spectra of all 36 linkers also has many overlapping signals, which are difficult to resolve in solution state NMR and would be impossible to distinguish in ssNMR, preventing an accurate measurement of the signal intensity.

The linkers of each MTV-MOF were calculated to be 75.0, 74.8, 75.1, and 75.1% of the total mass for I, II, III, and IV, respectively, compared to 63.9% for the BDC linker of MOF-5. This is evident in the TGA results, Figure 1d, which show greater weight percentages remaining at 600 °C for each MTV-MOF compared to MOF-5. This corresponds with the greater amount of carbon in the initial sample that remains after heating under a nitrogen atmosphere during the TGA measurement. The decomposition of MOF-5 shows a single step starting at 400 °C and finishing at 525 °C to give a total weight loss of 49.8%. All MTV-MOF-5 samples have a similar TGA decomposition profile, where each shows gradual weight loss until 200 °C, a steeper weight loss step between 200 and 400 °C, then the steepest weight loss between 400 and 500 °C. These results match what was previously observed for MTV-MOF-5 containing aromatic linkers, where the weight loss begins at 200 °C.[16] The total weight loss of each MTV-MOF is 41.1, 42.3, 38.9, and 42.1% for I, II, III, and IV, respectively, corresponding with a greater mass of zinc carbide remaining after heating compared to MOF-5.

All MTV-MOF-5 samples remain porous with 36 linkers, shown by type I nitrogen isotherms at 77 K in Figure 1e. The BET surface area and pore volume both decreased compared

https://doi.org/10.1021/acs.inorgchem.5c00015
Inorg. Chem. 2025, 64, 5561−5567

to MOF-5, which is expected from the presence of the large linker functionalities in the pores. Specifically, the BET surface areas are calculated to be 1,735, 1,755, 1,659, and 1,725 m^2/g for I, II, III, and IV, respectively, compared to 3,380 m^2/g for the MOF-5 sample. The cumulative pore volumes are 0.72, 0.72, 0.68, and 0.70 cm^3/g for I, II, III, and IV, respectively, compared to 1.37 cm^3/g for MOF-5. Pore sizes calculated by nonlocal density functional theory (Figures S19−S31) show broad pore size distributions centered from 7 to 10 Å for all MTV-MOFs, suggesting the presence of many different pore environments. Narrow pore size distributions, as is present for both MOF-5 pores with sizes of 8.4 and 13.6 Å, indicates the pore environments are nearly identical in each pore, which is expected when a single linker is used to construct the framework. The absence of a pore size near those of MOF-5 for each MTV-MOF indicates there are not large regions of linker A present in the crystal, suggesting it is well distributed throughout the MTV-MOF with the functionalized linkers.[16]

CONCLUSION

We successfully synthesized 4 MTV-MOF-5 structures with 36 different linkers incorporated to the backbone. These MTV-MOF-5 structures maintained their crystallinity and porosity despite the presence of many large functional groups in the pores of the MTV-MOFs. The final linker incorporations were calculated by integrating the solution state NMR of the digested frameworks despite many overlapping chemical shifts from the various linkers. 36 linkers into 12 possible locations around each pore results in almost 7.90×10^{17} different possible pore environments, more pores than are expected to exist in one crystal of MTV-MOF-5. A potential application of this system is to provide a scaffold with many different functionalized linkers to quickly identify the most promising linker or combination of linkers for another application of interest. This work demonstrates the excellent flexibility and tunability of MOFs by including a record number of linkers and functionalities into a single framework.

ASSOCIATED CONTENT

Supporting Information

The Supporting Information is available free of charge at https://pubs.acs.org/doi/10.1021/acs.inorgchem.5c00015.

Detailed experimental procedures, synthesis, and characterization details of the reported compounds, including digest NMR, PXRD, TGA, nitrogen sorption isotherms, and 11 linker MTV-MOF-5 linker incorporations (PDF)

AUTHOR INFORMATION

Corresponding Author

Omar M. Yaghi − *Department of Chemistry, University of California, Berkeley, California 94720, United States; Kavli Energy Nanoscience Institute and Bakar Institute of Digital Materials for the Planet, College of Computing, Data Science, and Society, University of California, Berkeley, California 94720, United States; KACST−UC Berkeley Center of Excellence for Nanomaterials for Clean Energy Applications, King Abdulaziz City for Science and Technology, Riyadh 11442, Saudi Arabia;* orcid.org/0000-0002-5611-3325; Email: yaghi@berkeley.edu

Authors

Matthew Burigana − *Department of Chemistry, University of California, Berkeley, California 94720, United States; Kavli Energy Nanoscience Institute and Bakar Institute of Digital Materials for the Planet, College of Computing, Data Science, and Society, University of California, Berkeley, California 94720, United States;* orcid.org/0009-0000-8708-4443

Haoze Wang − *Department of Chemistry, University of California, Berkeley, California 94720, United States; Kavli Energy Nanoscience Institute, University of California, Berkeley, California 94720, United States*

Jonas Elmroth Nordlander − *Department of Chemistry, University of California, Berkeley, California 94720, United States; Kavli Energy Nanoscience Institute, University of California, Berkeley, California 94720, United States*

Complete contact information is available at: https://pubs.acs.org/10.1021/acs.inorgchem.5c00015

Author Contributions

#M.B. and H.W. contributed equally to this work. The manuscript was written through contributions of all authors. All authors have given approval to the final version of the manuscript.

Funding

Funding for this project was provided by the King Abdulaziz City for Science and Technology.

Notes

The authors declare no competing financial interest.

ACKNOWLEDGMENTS

The authors acknowledge the King Abdulaziz City for Science and Technology for financial support of this project. The authors thank Dr. Jacopo Andreo and Prof. Stefan Wuttke at the Basque Center for Materials, Applications and Nanostructures for helpful discussions. The authors thank Drs. Hasan Celik, Raynald Giovine, and the Pines Magnetic Resonance Center's Core NMR Facility (PMRC Core) for spectroscopic assistance. An instrument used in this work was in part supported by NIH S10OD024998. The authors thank the Molecular Graphics and Computation Facility in the College of Chemistry at UC Berkeley, which is supported by NIH S10OD034382.

REFERENCES

(1) Yaghi, O. M.; Li, G.; Li, H. Selective Binding and Removal of Guests in a Microporous Metal−Organic Framework. *Nature* **1995**, *378* (6558), 703−706.

(2) Li, H.; Eddaoudi, M.; Groy, T. L.; Yaghi, O. M. Establishing Microporosity in Open Metal−Organic Frameworks: Gas Sorption Isotherms for Zn(BDC) (BDC = 1,4-Benzenedicarboxylate). *J. Am. Chem. Soc.* **1998**, *120* (33), 8571−8572.

(3) Li, H.; Eddaoudi, M.; O'Keeffe, M.; Yaghi, O. M. Design and Synthesis of an Exceptionally Stable and Highly Porous Metal-Organic Framework. *Nature* **1999**, *402* (6759), 276−279.

(4) Seki, K. Design of an Adsorbent with an Ideal Pore Structure for Methane Adsorption Using Metal Complexes. *Chem. Commun.* **2001**, No. 16, 1496−1497.

(5) Ma, B.-Q.; Mulfort, K. L.; Hupp, J. T. Microporous Pillared Paddle-Wheel Frameworks Based on Mixed-Ligand Coordination of Zinc Ions. *Inorg. Chem.* **2005**, *44* (14), 4912−4914.

(6) Koh, K.; Wong-Foy, A. G.; Matzger, A. J. A Crystalline Mesoporous Coordination Copolymer with High Microporosity. *Angew. Chem., Int. Ed.* **2008**, *47* (4), 677−680.

(7) Koh, K.; Wong-Foy, A. G.; Matzger, A. J. A Porous Coordination Copolymer with over 5000 M2/g BET Surface Area. *J. Am. Chem. Soc.* **2009**, *131* (12), 4184−4185.
(8) Furukawa, H.; Ko, N.; Go, Y. B.; Aratani, N.; Choi, S. B.; Choi, E.; Yazaydin, A. Ö.; Snurr, R. Q.; O'Keeffe, M.; Kim, J.; Yaghi, O. M. Ultrahigh Porosity in Metal-Organic Frameworks. *Science* **2010**, *329* (5990), 424−428.
(9) Liu, L.; Konstas, K.; Hill, M. R.; Telfer, S. G. Programmed Pore Architectures in Modular Quaternary Metal−Organic Frameworks. *J. Am. Chem. Soc.* **2013**, *135* (47), 17731−17734.
(10) Dutta, A.; Wong-Foy, A. G.; Matzger, A. J. Coordination Copolymerization of Three Carboxylate Linkers into a Pillared Layer Framework. *Chem. Sci.* **2014**, *5* (10), 3729−3734.
(11) Banerjee, R.; Phan, A.; Wang, B.; Knobler, C.; Furukawa, H.; O'Keeffe, M.; Yaghi, O. M. High-Throughput Synthesis of Zeolitic Imidazolate Frameworks and Application to CO2 Capture. *Science* **2008**, *319* (5865), 939−943.
(12) Phan, A.; Doonan, C. J.; Uribe-Romo, F. J.; Knobler, C. B.; O'Keeffe, M.; Yaghi, O. M. Structure, and Carbon Dioxide Capture Properties of Zeolitic Imidazolate Frameworks. *Acc. Chem. Res.* **2010**, *43* (1), 58−67.
(13) Wu, T.; Bu, X.; Zhang, J.; Feng, P. New Zeolitic Imidazolate Frameworks: From Unprecedented Assembly of Cubic Clusters to Ordered Cooperative Organization of Complementary Ligands. *Chem. Mater.* **2008**, *20* (24), 7377−7382.
(14) Banerjee, R.; Furukawa, H.; Britt, D.; Knobler, C.; O'Keeffe, M.; Yaghi, O. M. Control of Pore Size and Functionality in Isoreticular Zeolitic Imidazolate Frameworks and Their Carbon Dioxide Selective Capture Properties. *J. Am. Chem. Soc.* **2009**, *131* (11), 3875−3877.
(15) Furukawa, H.; Müller, U.; Yaghi, O. M. Heterogeneity within Order" in Metal−Organic Frameworks. *Angew. Chem., Int. Ed.* **2015**, *54* (11), 3417−3430.
(16) Deng, H.; Doonan, C. J.; Furukawa, H.; Ferreira, R. B.; Towne, J.; Knobler, C. B.; Wang, B.; Yaghi, O. M. Multiple Functional Groups of Varying Ratios in Metal-Organic Frameworks. *Science* **2010**, *327* (5967), 846−850.
(17) Rosi, N. L.; Kim, J.; Eddaoudi, M.; Chen, B.; O'Keeffe, M.; Yaghi, O. M. Rod Packings and Metal−Organic Frameworks Constructed from Rod-Shaped Secondary Building Units. *J. Am. Chem. Soc.* **2005**, *127* (5), 1504−1518.
(18) Wang, L. J.; Deng, H.; Furukawa, H.; Gándara, F.; Cordova, K. E.; Peri, D.; Yaghi, O. M. Synthesis and Characterization of Metal−Organic Framework-74 Containing 2, 4, 6, 8, and 10 Different Metals. *Inorg. Chem.* **2014**, *53* (12), 5881−5883.
(19) Lee, S.; Bürgi, H.-B.; Alshmimri, S. A.; Yaghi, O. M. Impact of Disordered Guest−Framework Interactions on the Crystallography of Metal−Organic Frameworks. *J. Am. Chem. Soc.* **2018**, *140* (28), 8958−8964.
(20) Osborn Popp, T. M.; Plantz, A. Z.; Yaghi, O. M.; Reimer, J. A. Precise Control of Molecular Self-Diffusion in Isoreticular and Multivariate Metal-Organic Frameworks. *ChemPhyschem* **2020**, *21* (1), 32−35.
(21) Kong, X.; Deng, H.; Yan, F.; Kim, J.; Swisher, J. A.; Smit, B.; Yaghi, O. M.; Reimer, J. A. Mapping of Functional Groups in Metal-Organic Frameworks. *Science* **2013**, *341* (6148), 882−885.

https://doi.org/10.1021/acs.inorgchem.5c00015
Inorg. Chem. 2025, 64, 5561−5567